iScience, Volume *23*

Supplemental Information

Flexible Multiplexed In_2O_3 Nanoribbon Aptamer-Field-Effect Transistors for Biosensing

Qingzhou Liu, Chuanzhen Zhao, Mingrui Chen, Yihang Liu, Zhiyuan Zhao, Fanqi Wu, Zhen Li, Paul S. Weiss, Anne M. Andrews, and Chongwu Zhou

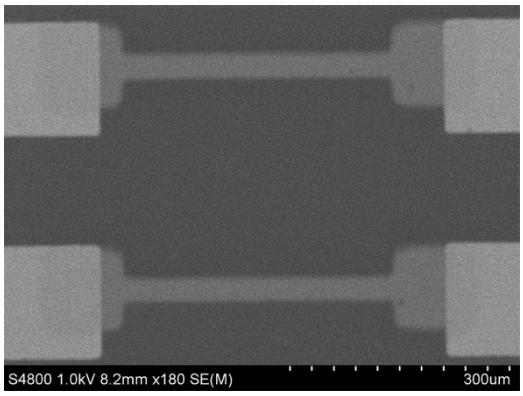

Figure S1. Scanning electron microscope image of two In_2O_3 nanoribbon field-effect transistors on a polyethylene terephthalate substrate. Each nanoribbon has a length of 500 μm and a width of 25 μm. Related to **Figure 1**.

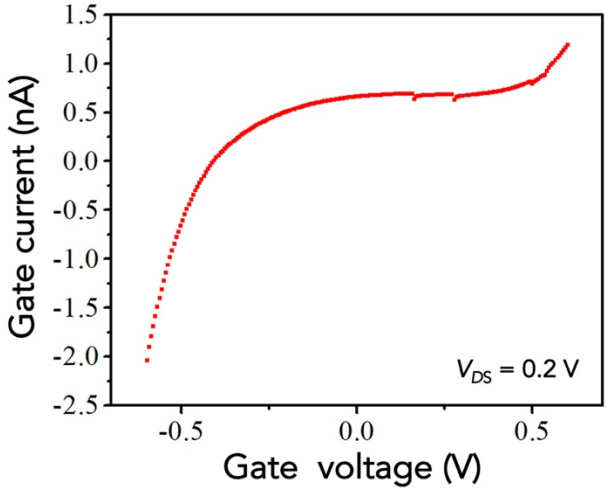

Figure S2. Gate leakage current *vs.* gate voltage from a representative In_2O_3 FET using a Au common gate. The gate leakage was negligible, and as shown, was smaller than 2 nA at V_{DS}=0.2 V. Related to **Figure 2**.

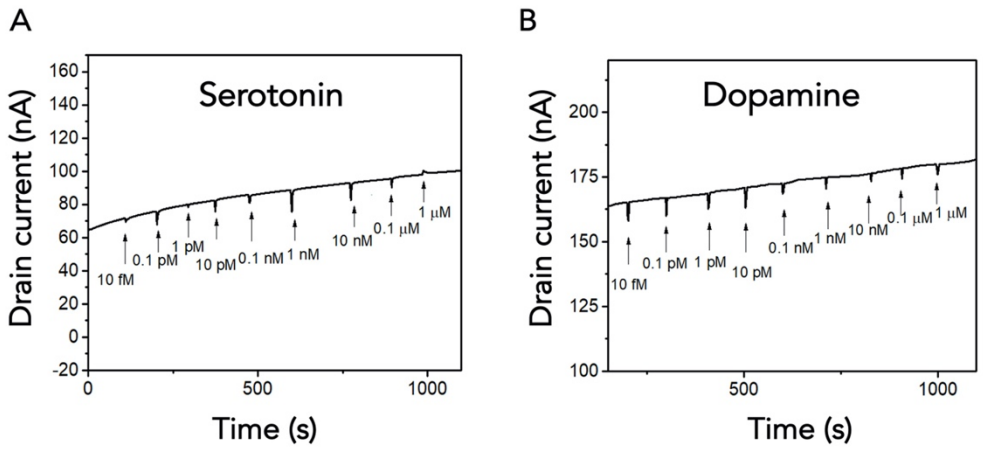

Figure S3. Control experiments for serotonin and dopamine sensing. The same sensing procedure was used at that in Figure 4 in the main text except sensors lacked (A) serotonin aptamers and (B) dopamine aptamers. Related to **Figure 4**.

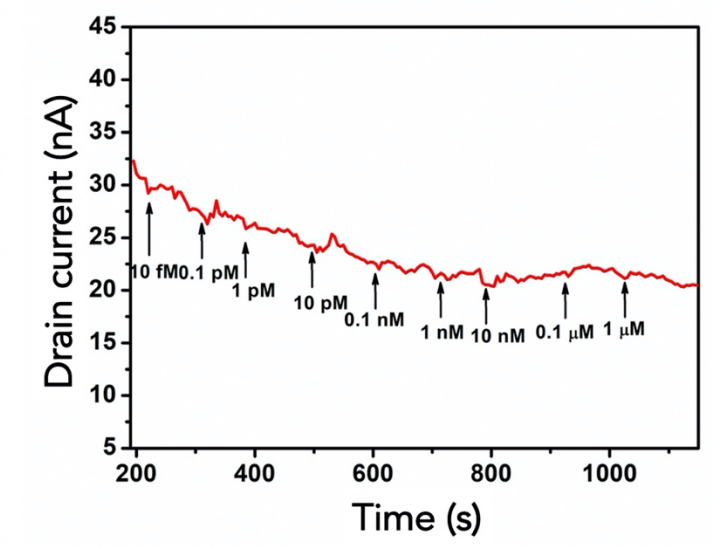

Figure S4. Control experiment with scrambled serotonin aptamer sequence for serotonin sensing.

Related to **Figure 4**.

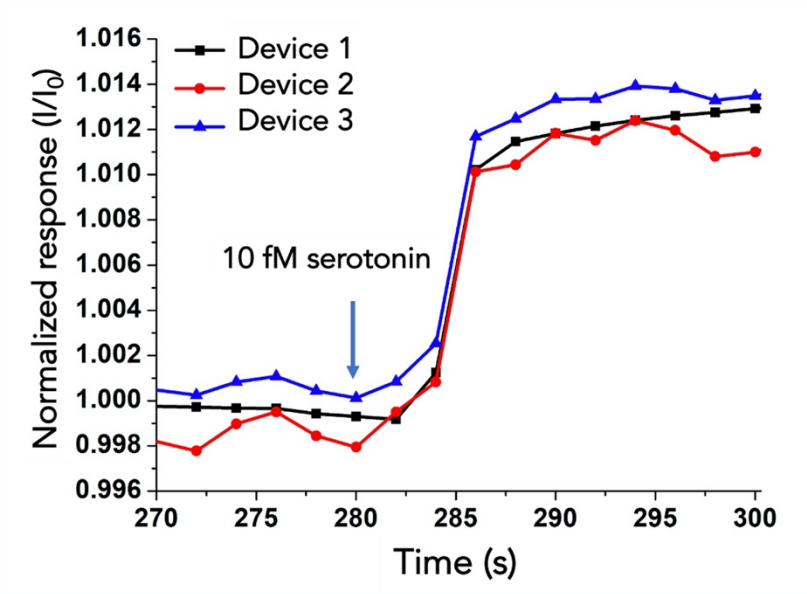

Figure S5. Temporal responses of In_2O_3 nanoribbon FETs to addition of 100 fM serotonin. Data are the same as those shown in Figure 4b in main text but are graphed to focus on temporal resolution for target sensing. Related to **Figure 4**.

Transparent Methods

Mobility calculation

The charge-carrier mobility of the In_2O_3 nanoribbon FETs is estimated using the following equation:

$$g_m = \frac{dI_D}{dV_{GS}} = \frac{W}{L} \cdot C_{DL} \cdot \mu_{FE} \cdot V_{DS}$$

where W is the channel width, L is the channel length, and C_{DL} is the electrical double layer capacitance per unit area in 0.1 M ionic strength aqueous solution (phosphate-buffered saline), reported previously as 25.5 μF cm^{-2} (Park et al., 2015). The maximum transconductance of 4.77 μS was obtained at a drain voltage of 0.2 V and a gate voltage of 0.43 V. The corresponding mobility is 18.7 cm^2 V^{-1} s^{-1}.

Tensile strain calculation

To calculate tensile strain when In_2O_3 nanoribbon FETs were wrapped tightly around a copper wire with a radius ~ 0.1 mm, we used the following formula:

$$\varepsilon = \frac{1}{R} \times \frac{d_s + d_f}{2} \times \frac{\chi \cdot \gamma^2 + 2 \cdot \chi \cdot \gamma + 1}{\chi \cdot \gamma^2 + \chi \cdot \gamma + \gamma + 1}$$

Here, R is the bending radius, d_s is the thickness of the substrate, d_f is the thickness of the In_2O_3 nanoribbon, $\gamma = d_f / d_s$ and $\chi = Y_f / Y_s$, where Y_f and Y_s are the Young's moduli of the In_2O_3 FET and substrate, respectively. If we assume $Y_f = Y_s$, the above equation can be simplified to:

$$\varepsilon = \frac{1}{R} \times \frac{d_s + d_f}{2}$$

The thickness of the polyethylene terephthalate (PET) substrate is 1.4 μm and the total thickness of the FET is less than 100 nm. With a bending radius of 0.1 mm, the tensile strain is calculated to be ~ 0.75 %.

Materials

All chemicals were purchased from Sigma-Aldrich Co. (St. Louis, MO), unless otherwise noted below. The SYLGARD 184 for fabricating polydimethylsiloxane (PDMS) wells and brain mimics was from Dow Corning Corporation (Midland, MI). Brain mimics were produced using silicone brain molds (Amazon #B003AQB2XK). The PDMS wells were made by cutting holes (~5 mm) in 3-mm PDMS sheets. The 1.4-μm-thick polyethylene terephthalate (PET) substrates were purchased from DuPont Teijin Films (Chester, VA) and used as received. Film thicknesses were measured and determined by the vendor using dielectric strength.

Physiological phosphate-buffered saline contained 137 mM NaCl, 2.7 mM KCl, 10 mM Na_2HPO_4, 1.8 mM KH_2PO_4. Artificial cerebrospinal fluid contained 147 mM NaCl, 3.5 mM KCl, 1 mM NaH_2PO_4, 2.5 mM $NaHCO_3$, 1 mM $CaCl_2$, and 1.2 mM $MgCl_2$. Oligonucleotides were obtained from Integrated DNA Technologies (Coralville, IA). Serotonin aptamer: 5'-/5ThioMC6-D/CGACTGGTAGGCAGATAGGGGAA GCTGATTCGATGCGTGGGTCG-3'. Serotonin scrambled aptamer: 5'-/5ThioMC6-D/CCCGG GAATTCCGGAATTGGGGCAATTGATGAGGGGGTCATGGG-3'. Dopamine aptamer: 5'-/5ThioMC6-D/CGACGCCAGTTTGAAGGTTCGTTCGCAGGTGTGGAGTGACGTCG-3'.

Device fabrication

Each 1.4-μm-thick PET film was attached to a rigid carrier wafer *via* a PDMS adhesion layer. The lamination was performed by attaching a corner of each PET film to a sacrificial PDMS layer, then aligning the edges. A soft scraper was used to smooth the attached film and to remove any bubbles. After immersing in consecutive acetone and isopropanol rinses for 15 min each, the first shadow mask was attached to each substrate to define the In_2O_3 nanoribbons. The In_2O_3 was deposited by RF sputtering (Denton Discovery 550 sputtering system). The nanoribbon thickness was controlled by the sputtering time. An In_2O_3 thickness of 16 nm was selected for all devices because this was the thinnest In_2O_3 layer that could be sputtered to give consistent device performance and high sensitivities to ion concentrations, *e.g.*, pH (Aroonyadet et al., 2015). Nanoribbon FETs with the same width and different thicknesses have been compared, where thinner nanoribbon FETs with higher surface-to-volume ratios showed the highest sensitivity to pH (Aroonyadet, et al., 2015).

The source, drain, and common gate electrodes, and temperature sensors were patterned using a second shadow mask. The bottom 1-nm Ti and top 50-nm Au layers were deposited *via* electron-beam (e-beam) evaporation. Device arrays were then peeled from their carrier wafers. Metal films deposited by e-beam evaporation were patterned using shadow masks, which is a cost-effective, cleanroom-free, and high-throughput process (Aroonyadet, et al., 2015; Liu et al., 2018). Moreover, this process does not result in In_2O_3 photoresist contamination or chemical exposure (Aroonyadet, et al., 2015). The thickness of the electrode metal layers impacts their performance. Previous studies indicated that the use of Au at 10-50 nm with a Ti adhesion layer of <5 nm provides robust flexibility with minimal cracking (Adrega et al., 2010; Seghir et al., 2015; Baetens et al., 2018). Graphene is another electrode candidate for flexible electronics. Graphene has been

deposited as a liquid-based mat and patterned by ink-jet printing or photolithography, the latter of which requires cleanroom processing and chemical exposure associated with the use of photoresist (Liu et al., 2014; Yang et al., 2016; Han et al., 2017; Song et al., 2017). Other conductive metal oxides that have been used for electrodes, such as indium-tin-oxide or fluorine-doped tin-oxide (Spechler et al., 2015; Yang, et al., 2016), have similar chemical properties as the channel material used here, *i.e.*, In_2O_3, which makes it challenging to functionalize channel regions separately from electrodes.

Surface functionalization

(3-Aminopropyl)trimethoxysilane and trimethoxy(propyl)silane 1:9 (v/v) were thermally evaporated using vapor-phase deposition onto In_2O_3 surfaces at 40 °C for 1 h followed by incubation in 1 mM ethanolic 1-dodecanethiol for 1 h to passivate Au electrodes. Substrates were rinsed in ethanol and immersed in 1 mM solutions of 3-maleimidobenzoic acid *N*-hydroxysuccinimide ester (MBS) dissolved in a 1:9 (v/v) mixture of dimethyl sulfoxide and PBS for 30 min. The MBS crosslinks amine-terminated silanes with thiolated DNA aptamers (Nakatsuka et al., 2018).

Aptamers (1 mM in nuclease-free water) were stored at -20 °C and diluted to 1 µM in nuclease-free water. Aptamers were heated for 5 min at 95 °C and cooled in an ice bath to room temperature. Substrates were rinsed with deionized water and immersed in 1 µM solutions of thiolated DNA aptamers overnight (~18 h), rinsed again with deionized water, and blown dry with N_2 gas before measurements. For multiplexed measurements, serotonin and dopamine aptamers (50 µL each) were added using a pipette onto two different adjacent devices. One FET on the

serotonin device was covered by a PDMS mask before adding the aptamer solution. The mask was then removed to expose an unfunctionalized FET, which served as a pH sensor.

Measurements

Each FET was connected with indium wires for electronic measurements. For the crumpling test, device arrays were crumpled tightly and held crumpled using tweezers for each crumpling cycle as shown in Fig. 3b. After ~5 s of crumpling, each array was then flattened. The crumpling and flattening cycles were repeated 100 times. Data were collected after 5, 10, 50, and 100 crumpling cycles. The concentrations of serotonin and dopamine tested were selected based on estimates of *in vivo* extracellular concentrations from our previous *in vivo* microdialysis measurements (Mathews et al., 2004; Yang et al., 2013; Yang et al., 2015). For multiplexed sensing, after using indium wires to connect the bonding pads of each FET, pH, serotonin, dopamine, and temperature sensors were covered with aCSF or different neurotransmitter solutions. Electrical characteristics under ambient conditions for the In_2O_3 FET devices were measured using an Agilent 4156B precision semiconductor parameter analyzer. Electrical characteristics in buffer and sensing results were measured with an Agilent B1500 semiconductor analyzer with capability to measure eight FETs at the same time (Ishikawa et al., 2009; Chang et al., 2011). Testing solutions of 300 μL were added to the PDMS wells. After each measurement, solutions were quickly removed using one pipette and the next testing solution was added immediately using a second pipette.

Supplemental references

Adrega, T.; Lacour, S. P. (2010). Stretchable gold conductors embedded in PDMS and patterned by photolithography: Fabrication and electromechanical characterization. *J. Micromech. Microeng. 20*, 055025.

Aroonyadet, N.; Wang, X.; Song, Y.; Chen, H.; Cote, R. J.; Thompson, M. E.; Datar, R. H.; Zhou, C. (2015). Highly scalable, uniform, and sensitive biosensors based on top-down indium oxide nanoribbons and electronic enzyme-linked immunosorbent assay. *Nano Lett. 15*, 1943–1951.

Baetens, T.; Pallecchi, E.; Thomy, V.; Arscott, S. (2018). Cracking effects in squashable and stretchable thin metal films on PDMS for flexible microsystems and electronics. *Sci. Rep. 8*, 9492.

Chang, H. K.; Ishikawa, F. N.; Zhang, R.; Datar, R.; Cote, R. J.; Thompson, M. E.; Zhou, C. (2011). Rapid, label-free, electrical whole blood bioassay based on nanobiosensor systems. *ACS Nano 5*, 9883–9891.

Han, T.-H.; Kim, H.; Kwon, S.-J.; Lee, T.-W. (2017). Graphene-based flexible electronic devices. *Mater. Sci. Eng. R Rep. 118*, 1–43.

Ishikawa, F. N.; Curreli, M.; Chang, H. K.; Chen, P. C.; Zhang, R.; Cote, R. J.; Thompson, M. E.; Zhou, C. (2009). A calibration method for nanowire biosensors to suppress device-to-device variation. *ACS Nano 3*, 3969–3976.

Liu, Q.; Liu, Y.; Wu, F.; Cao, X.; Li, Z.; Alharbi, M.; Abbas, A. N.; Amer, M. R.; Zhou, C. (2018). Highly sensitive and wearable In_2O_3 nanoribbon transistor biosensors with integrated on-chip gate for glucose monitoring in body fluids. *ACS Nano 12*, 1170–1178.

Liu, Y.; Zhou, H.; Cheng, R.; Yu, W.; Huang, Y.; Duan, X. (2014). Highly flexible electronics from scalable vertical thin film transistors. *Nano Lett. 14*, 1413–1418.

Mathews, T. A.; Fedele, D. E.; Coppelli, F. M.; Avila, A. M.; Murphy, D. L.; Andrews, A. M. (2004). Gene dose-dependent alterations in extraneuronal serotonin but not dopamine in mice with reduced serotonin transporter expression. *J. Neurosci. Methods 140*, 169–181.

Nakatsuka, N.; Yang, K. A.; Abendroth, J. M.; Cheung, K. M.; Xu, X.; Yang, H.; Zhao, C.; Zhu, B.; Rim, Y. S.; Yang, Y., et al. (2018). Aptamer-field-effect transistors overcome Debye length limitations for small-molecule sensing. *Science 362*, 319–324.

Park, S.; Lee, S.; Kim, C.-H.; Lee, I.; Lee, W.-J.; Kim, S.; Lee, B.-G.; Jang, J.-H.; Yoon, M. H. (2015). Sub-0.5 V highly stable aqueous salt gated metal oxide electronics. *Sci. Rep. 5*, 13088.

Seghir, R.; Arscott, S. (2015). Controlled mud-crack patterning and self-organized cracking of polydimethylsiloxane elastomer surfaces. *Sci. Rep. 5*, 14787.

Song, D.; Mahajan, A.; Secor, E. B.; Hersam, M. C.; Francis, L. F.; Frisbie, C. D. (2017). High-resolution transfer printing of graphene lines for fully printed, flexible electronics. *ACS Nano 11*, 7431–7439.

Spechler, J. A.; Koh, T.-W.; Herb, J. T.; Rand, B. P.; Arnold, C. B. (2015). A transparent, smooth, thermally robust, conductive polyimide for flexible electronics. *Adv. Funct. Mater. 25*, 7428–7434.

Yang, H.; Thompson, A. B.; McIntosh, B. J.; Altieri, S. C.; Andrews, A. M. (2013). Physiologically relevant changes in serotonin resolved by fast microdialysis. *ACS Chem. Neurosci. 4*, 790–798.

Yang, H.; Sampson, M. M.; Senturk, D.; Andrews, A. M. (2015). Sex- and SERT-mediated differences in stimulated serotonin revealed by fast microdialysis. *ACS Chem. Neurosci. 6*, 1487–1501.

Yang, W.; Wang, C. (2016). Graphene and the related conductive inks for flexible electronics. *J. Mater. Chem. C 4*, 7193–7207.